Talanta 94 (2012) 335–341

Contents lists available at SciVerse ScienceDirect

Talanta

journal homepage: www.elsevier.com/locate/talanta

Spectrometric analysis of process etching solutions of the photovoltaic industry—Determination of HNO_3, HF, and H_2SiF_6 using high-resolution continuum source absorption spectrometry of diatomic molecules and atoms

Stefan Bücker, Jörg Acker*

Hochschule Lausitz (FH) – University of Applied Sciences, Faculty of Natural Sciences, Department of Chemistry, Großenhainer Straße 57, D-01968 Senftenberg, Germany

ARTICLE INFO

Article history:
Received 29 November 2011
Received in revised form 7 March 2012
Accepted 20 March 2012
Available online 2 April 2012

Keywords:
Molecular absorption spectrometry (MAS)
Atomic absorption spectrometry (AAS)
Aluminum mono-fluoride (AlF)
Nitrous monoxide (NO)
$HF–HNO_3$ etch solution
H_2SiF_6
Silicon
Texturization
High-resolution continuum source atomic absorption spectrometer

ABSTRACT

The surface of raw multicrystalline silicon wafers is treated with $HF–HNO_3$ mixtures in order to remove the saw damage and to obtain a well-like structured surface of low reflectivity, the so-called texture. The industrial production of solar cells requires a consistent level of texturization for tens of thousands of wafers. Therefore, knowing the actual composition of the etch bath is a key element in process control in order to maintain a certain etch rate through replenishment of the consumed acids.

The present paper describes a novel approach to quantify nitric acid (HNO_3), hydrofluoric acid (HF), and hexafluosilicic acid (H_2SiF_6) using a high-resolution continuum source graphite furnace absorption spectrometer. The concentrations of Si (via Si atom absorption at the wavelength 251.611 nm, $m_{0,Si}$ = 130 pg), of nitrate (via molecular absorption of NO at the wavelength 214.803 nm, m_{0,NO_3^-} = 20 ng), and of total fluoride (via molecular absorption of AlF at the wavelength 227.46 nm, $m_{0,F}$ = 13 pg) were measured against aqueous standard solutions. The concentrations of H_2SiF_6 and HNO_3 are directly obtained from the measurements. The HF concentration is calculated from the difference between the total fluoride content, and the amount of fluoride bound as H_2SiF_6. H_2SiF_6 and HNO_3 can be determined with a relative uncertainty of less than 5% and recoveries of 97–103% and 96–105%, respectively. With regards to HF, acceptable results in terms of recovery and uncertainty are obtained for HF concentrations that are typical for the photovoltaic industry. The presented procedure has the unique advantage that the concentration of both, acids and metal impurities in etch solutions, can be routinely determined by a single analytical instrument.

1. Introduction

Chemical etching of silicon with mixtures of $HF–HNO_3$ is an essential step in the processing of solar grade silicon, removing the mechanically damaged surface of silicon wafers after slicing from ingots (saw damage) and texturing the silicon wafers to obtain low reflective surfaces. In this process, HNO_3 and HF are consumed, and H_2SiF_6 is formed as the major reaction product in the etch solution. This process is described in literature [1] by the following net equation (Eq. (1)); however, recent results have shown that the reaction is more complex [2,3].

$$3Si + 18HF + 4HNO_3 \rightarrow 3H_2SiF_6 + 4NO + 8H_2O \quad (1)$$

The parameters of etching are mainly determined by the concentrations of HF and HNO_3 as well as the amount of dissolved silicon [2]. The concentration of H_2SiF_6 in particular has a significant impact on the texture and the reflectivity of etched multicrystalline wafers [4]. Thus, the concentrations of HF, H_2SiF_6, and HNO_3 in industrial etch lines have to be kept in narrow margins to produce solar cells of consistent efficiency. In the past, numerous methods were developed to determine the acid concentrations. Henßge et al. [5,6] developed a procedure to quantify HF, H_2SiF_6, and HF in the same sample by titration in aqueous and non-aqueous media. Another, much faster method based on ion chromatography was presented by Acker and Henßge [7]. Zimmer et al. [8,9] combined the latter method with a postcolumn derivatization to determine silicon directly through UV detection. Finally, a NIR technique can be used to monitor the etch bath constituents [10,11]. This technique is reputed to be time and cost saving; the calibration process, however, is difficult and time consuming.

The present work was inspired by measurements of metal ion concentrations in industrial etch solutions. The sawing process,

Abbreviations: ET-HR-CS MAS, high-resolution continuum source molecular absorption spectrometry in an electro-thermal heated graphite furnace; ET-HR-CS AAS, high-resolution continuum source atomic absorption spectrometry in an electro-thermal heated graphite furnace.

* Corresponding author. Tel.: +49 3573 85 839; fax: +49 3573 85 809.
E-mail address: joerg.acker@hs-lausitz.de (J. Acker).

0039-9140/$ – see front matter © 2012 Elsevier B.V. All rights reserved.
http://dx.doi.org/10.1016/j.talanta.2012.03.052

using a SiC slurry and a metal wire, leaves metallic contaminations on the silicon surface which are not fully removed by the post-sawing cleaning processes. Therefore, the metal ion concentrations (typically in the range between 0.01 and 0.4 ppm) as well as the concentrations of HF, HNO_3, and H_2SiF_6 have to be determined at regular intervals. Both types of analysis can be carried out routinely and with minimal sample preparation by means of a high-resolution continuum source atomic absorption spectrometer.

Since the determination of metal ions with high-resolution continuum source atomic absorption spectrometry (HR-CS AAS) has become an established procedure, the present paper only deals with the determination of the acid concentrations. Therefore, the determination of silicon by its atomic absorption was optimized for this specific purpose. The determination of the non-metals fluoride and nitrogen requires that the element is converted into a diatomic molecule of sufficient stability, life time and concentration in order to become detectable. The diatomic analyte molecule consists of one non-metal element atom and one reagent atom. The reagent is usually added to the analyte solution as an easily soluble compound.

Using a high-resolution continuum source spectrometer, it has been shown for fluorine [12–14], chlorine [12], bromine [15], iodine [16], phosphorus [12,17], and sulfur [12,18] that suitable diatomic analyte molecules of these elements are formed during a sample heating procedure in a graphite furnace. Huang et al. [19] recently used the molecular absorption of NO at the wavelength of 215.360 nm to determine nitrate in ground water (CRM 616 und CRM 617) and in an aqueous solution of calcium ammonium nitrate fertilizer (BCR 178) in a graphite furnace with a PIN platform. A LOD of 5 ng nitrogen (0.25 mg L^{-1}) was reached using 50 μg calcium as modifier (added to the sample as $CaCl_2$). The procedure is suitable for nitrate solutions, nitric acid, or a nitrate solution in diluted acids with a higher volatility than nitric acid. However, in the presence of a less volatile acid compared to HNO_3, the NO molecular absorbance decreases dramatically for the given optimum pyrolysis temperature of 300 °C.

Applications to determine the total fluoride through molecular absorption spectrometry (MAS) in a graphite furnace have been known for decades. A determination can be carried out via the molecular absorption of GaF [12–14,20–29], InF [20–28], TlF [20], MgF [21–24,30–32], CaF [24,30,31] SrF [24,30,31], and BaF [24,30,31]. Regarding AlF, in the majority of cases, the molecular absorption at the wavelength of 227.45 nm was used [20–29,33–54], and a platinum or a cobalt hollow cathode, or a deuterium lamp was applied as excitation source.

Besides aluminum as reagent, several different cations, such as sodium [20], iron (III) [27] strontium [33–38], and barium [23,28,29,39–42], as well as mixtures of cations, like strontium and nickel (II) [43–47], strontium in combination with iron (III) [24–26,48–50], or ammonium [33] were added as chemical modifiers to enhance the molecular absorption of AlF and to decrease the background absorption. So far, the lowest characteristic mass of 20 pg fluoride was reported by Tsunoda et al. [27] using 2.7 μg of reagent (aluminum) and 5.6 μg of iron (III) as modifier in a Massman type graphite furnace. Overviews of these and other methods of molecular absorption spectrometry are provided by Welz et al. [55] and Dittrich [56,57].

The presented publication describes a new analytical procedure which allows the determination of nitrate via the molecular absorption of NO in silicon etching solutions of the photovoltaic industry and the adaption of well known methods, such as the silicon determination via its atomic absorption and the fluorine determination via the molecular absorption of AlF, to the analysis of etching solutions of the photovoltaic industry.

Table 1
Graphite furnace temperature program for silicon determination by means of AAS of Si at 251.611 nm.

	Temperature [°C]	Ramp [°C/s]	Hold time [s]	Argon flow
Injection of sample (20 μL) and modifier (8 μg Pd^{2+} and 4 μg Mg^{2+} as nitrates)				
Crying	80	6	20	Max.
Crying	90	3	20	Max.
Pyrolysis	350	50	20	Max.
Pyrolysis	1200	300	10	Max.
Auto zero	1200	0	5	Stopp.
Atomization	2550	1500	3	Stopp.
Cleaning	2600	250	6	Max.

Table 2
Graphite furnace temperature program for nitrate determination by means of MAS of NO at 214.803 nm.

	Temperature [°C]	Ramp [°C/s]	Hold time [s]	Argon flow
Injection of sample (20 μL) and modifier (68 μg La^{3+} as $LaCl_3$)				
Drying	100	2	15	Max.
Pyrolysis	200	5	7	Max.
Auto zero	200	0	5	Stopp.
Vaporization	950	1500	5	Stopp.
Cleaning	2550	250	6	Max.
Cooling	200	no power	2	Max.

2. Experimental

2.1. Instrumentation

A model contrAA 700 high resolution continuum source atomic absorption spectrometer (Analytik Jena AG, Jena, Germany) equipped with a transversely heated graphite tube atomizer and a flame atomizer, a 300 W xenon short-arc lamp (in a hot-spot mode) as continuum radiation source, a double monochromator consisting of a prism and an Echelle grating, and a linear charge coupled device detector were used for all absorption measurements carried out in the presented work. A detailed discussion of the instrument has been provided by Welz et al. [58].

All measurements were conducted using pyrolytically coated graphite furnaces without a PIN platform. The absorbances of the analyte species were recorded at the following wavelengths: AlF at 227.460 nm, silicon at 251.611 nm, and NO at 214.803 nm. The detector pixel at maximum absorption (central pixel) plus one neighboring pixel on each side of the central pixel were summarized to gain the signal value, which was further integrated in peak area mode. The oven programs used are summarized for the atomic absorption spectrometry (AAS) of silicon in Table 1, for the MAS of NO in Table 2, and for the MAS of AlF in Table 3.

Unless otherwise stated, all chemicals were supplied by Merck in p.a. quality. The calibrations were performed using single element standards obtained from dilution of 1000 ppm standard solutions (NH_4SiF_6, $NaNO_3$ and NaF in water) with the exception

Table 3
Graphite furnace temperature program of total fluoride determination by means of MAS of AlF at 227.460 nm.

	Temperature [°C]	Ramp [°C/s]	Hold time [s]	Argon flow
Injection of reagent (8 μg Al^{3+} as $Al(NO_3)_3$)				
Drying	70	1	0	Max.
Drying	110	2	3	Max.
Injection of sample (6 μL) and modifier (8 μg Ba^{2+} as $Ba(NO_3)_2$)				
Drying	70	1	0	Max.
Drying	110	2	3	Max.
Pyrolysis	600	40	15	Max.
Auto zero	600	0	5	Stopp.
Vaporization	2100	1500	5	Stopp.
Cleaning	2450	100	3	Max.

Table 4
Dilution factors for the samples used.

Sample	Silicon		Nitrate		Fluoride	
	AAS	ICP-OES	MAS	IC	MAS	IC
1	62,400	7300	1090	34,900	370,000	34,900
2	40,500	1890	1050	23,000	416,000	23,000
3	33,500	1300	1320	19,300	318,000	19,300
4	38,900	4700	920	31,800	315,000	31,800
5	62,900	7300	1110	34,800	440,000	34,800
Real sample	37,000	6700	1150	30,500	308,000	30,500

Table 5
ICP-OES measuring conditions.

Viewing mode	Axial
Generator power (W)	1150
Ar cooling flow (L min^{-1})	12
Ar auxiliary flow (L min^{-1})	0.5
Ar nebulizer flow (L min^{-1})	0.5
Maximum integration time (s)	20
Sample rinsing time (s)	5
Pump speed (rpm)	50
Repeating measurements	3

of AlF MAS, which is calibrated using a diluted hydrofluoric acid. The lanthanum modifier (c_{La} = 11 g L^{-1}) was prepared by dissolving $LaCl_3{\cdot}7H_2O$. The palladium-/magnesium nitrate modifier (c_{Pd} = 1 g L^{-1}, c_{Mg} = 0.5 g L^{-1}) was made from a $Mg(NO_3)_2{\cdot}6H_2O$ (suprapur® quality, Merck, Darmstadt, Germany) solution with an added aliquot of a palladium nitrate stock solution (10% (w/w) $Pd(NO_3)_2$ in 10% (w/w) HNO_3, Sigma–Aldrich). 1000 ppm single element standard stock solutions were used as aluminum reagent ($Al(NO_3)_3$ in 0.5 m HNO_3) and barium modifier solutions ($Ba(NO_3)_2$ in 1% (w/w) HNO_3, Roth, Karlsruhe, Germany). The studies of chemical interference in the case of fluoride and silicon were carried out using single element standards made by diluting 1000 ppm stock solutions ($Al(NO_3)_3$ in 0.5 m HNO_3, $Fe(NO_3)_3$ in 0.5 m HNO_3, $Cu(NO_3)_2$ in 0.5 m HNO_3, $Ni(NO_3)_2$ in 0.5 m HNO_3, $Ca(NO_3)_2$ in 0.5 m HNO_3, $NaNO_3$ in 0.5 m HNO_3, and $Mg(NO_3)_2$ in 0.5 m HNO_3). For the interference studies in the nitrate determination, stock solutions were made by dissolving $AlCl_3{\cdot}6H_2O$, $CaCl_2$, $FeCl_3{\cdot}6H_2O$, $Mg(OOCCH_3)_2$, NaCl, $CuCl_2$, and $NiCl_2{\cdot}6H_2O$ in high purity water.

All samples were measured in bracketing mode to correct the time drift of the signals. The given analytical results represent the average of three individual sample dilutions, each of them measured three times, and the respective single standard deviation of these nine individual values.

2.2. Preparation of the synthetic etch mixtures

All synthetic etch solutions were made of high purity water (conductivity <0.050 S cm^{-1}) obtained from a model PURELAB classic high purity water system (ELGA Berkefeld GmbH, Celle, Germany). The acids used, HF (40%, w/w) and HNO_3 (69%, w/w), are products of Merck, Darmstadt, Germany, in p.a. quality. H_2SiF_6 (46%, w/w) in p.a. quality was provided by Fluorchemie Dohna, Dohna, Germany. From these acids, synthetic etch mixtures were prepared in five different ratios to cover the compositions of etching solutions relevant in the photovoltaic industry.

The only sample preparation step was the dilution of these samples according to the parameters given in Table 4. The single real process etching solution of the photovoltaic industry was analyzed and diluted likewise.

2.3. Analysis with IC and ICP-OES

2.3.1. Nitrate and total fluoride determination via ion chromatography [7]

The ion chromatographic measurements were performed with a 761 Compact IC, equipped with a suppressor system and conductivity detector (MetrohmAG, Herisau, Switzerland). A METROSEP ASupp4/5 Guard (Metrohm AG, Herisau, Switzerland; length 5 mm, diameter 4.0 mm) was used as precolumn and a METROSEP ASupp5 (Metrohm AG, Herisau, Switzerland; length 250 mm, diameter 4.0 mm) as separation column. A carbonate eluent was used at a constant eluent flow of 0.7 mL min^{-1}. The carbonate eluent for the IC was made by dissolving Na_2CO_3 and $NaHCO_3$ in degassed, deionized water with final concentrations of about 3.2 mmol L^{-1} and 1.0 mmol L^{-1}, respectively.

A sample volume of 0.25 mL was weighed in a flask. NaOH solution was added to the sample until the pH value reached approximately 9, and finally, the flask was filled to a mass of 100 g solution. This solution was diluted by a factor of 200, given through a SPE-H^+-ion exchange column (Macherey-Nagel GmbH & Co. KG, Düren, Germany) and injected into the ion chromatograph. The calibration was performed by means of aqueous standards, containing both nitrate and fluoride.

2.3.2. Determination of silicon by means of ICP-OES [6]

An iCap 6000 ICP-OES (Thermo Fisher scientific, Waltham, Massachusetts, USA), equipped with a Mira Mist nebulizer, and a HF resistant spray chamber was used to determine the total Si concentration in the etching solutions. The samples were diluted by a factor of 7000, adding 1% (w/w) HF and 1% (w/w) HNO_3 in the last dilution step, as well as to all standards. The calibration was performed against acid matched Si single element standards (Merck, NH_4SiF_6). The operation parameters of the instrument are summarized in Table 5. All samples were measured in bracketing mode. The given analytical results and standard deviations represent the mean of three individual sample dilutions, each of them measured three times.

3. Results and discussion

3.1. Development of the analytical procedures

3.1.1. Silicon determination

The Si atomic absorption was measured at the commonly used wavelength of 251.611 nm. Because of the high concentrations of silicon in the etch solutions, the less expensive wall atomization was utilized instead of a PIN platform furnace, which is commonly used for silicon determination [59]. The background correction was carried out automatically by the spectrometer software in the so-called dynamic mode with a reference measurement.

Silicon is usually measured in the presence of a palladium-/magnesium modifier (0.1% (w/w) palladium, 0.05% (w/w) magnesium) injected into the graphite furnace together with the samples and standards. A modifier is commonly used to achieve a higher sensitivity. In the present case, it is more important to shorten the temperature range of vaporization and atomization to obtain a sharp and highly reproducible signal. Adding 8 μL or more of the modifier mix would result in a narrow and stable silicon atom absorption signal. A further increase of the modifier mass does not improve the absorbance, as shown in Fig. 1. Consequently, an addition of 8 μL of the modifier solution, representing 8 μg palladium and 4 μg magnesium, was used in the further work. The best and most reproducible signal shapes were found for a pyrolysis temperature of 1200 °C and an atomization temperature of 2550 °C. With the newly developed furnace program and modifier regime, a characteristic mass of 130 pg silicon and a LOD of 3.2 ng silicon is reached. The linear working range spans up to 50 ng silicon.

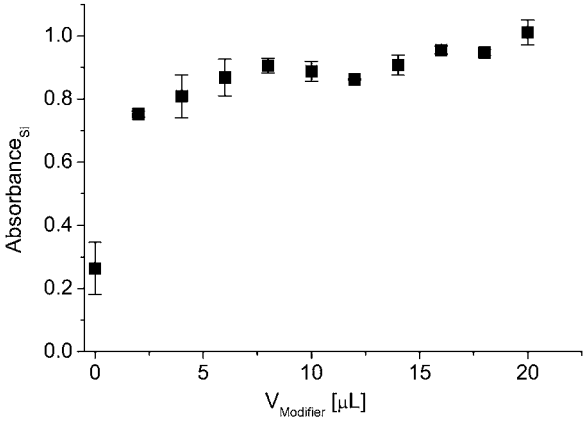

Fig. 1. Impact of the volume of the added palladium-/magnesium-nitrate modifier solution on the absorption of 20 ng silicon.

Another strategy in silicon determination is the pre-treatment of the modifier prior to the injection of the analyte into the graphite furnace. This route was tested, however, without any significant improvement of the signal shape and the absorbance.

No spectral interferences were found for calcium, aluminum, iron, nickel, copper, magnesium, and sodium, tested with a concentration of 5 mg L^{-1} in the diluted sample solution for the respective element (this corresponds to an unrealistically high concentration of at least 168 g L^{-1} in the undiluted sample solution). The elements mentioned represent the contaminations present in an industrial etching solution. Whereas nickel, copper, and magnesium have no impact on the silicon signal, the addition of calcium, iron, and sodium increases the silicon absorbance by approximately 15%; in case of aluminum by 40%. However, the discovered interference only occurs in the presence of these high concentrations. At metal ion concentrations of 170 µg L^{-1}, these interferences are not present. It should be noted that even these lower metal ion concentrations (corresponding to 5.6 g L^{-1} in the undiluted sample) are 180 times higher than those of real etch samples.

3.1.2. Nitrate determination

Although the nitrate concentration in etching solutions is very high, the application must be tuned to maximum sensitivity because the molecular absorption of NO is extremely insensitive. The spectrum of the most sensitive band system in the wavelength range of 213.0 nm to 215.5 nm is shown in Fig. 2. The absorption peaks shown are assigned to electronic transitions from the ground state to the 1st excited state and $\Delta v = +1$ ($X^2\Pi \rightarrow A^2\Sigma+$, v: $0 \rightarrow 1$)

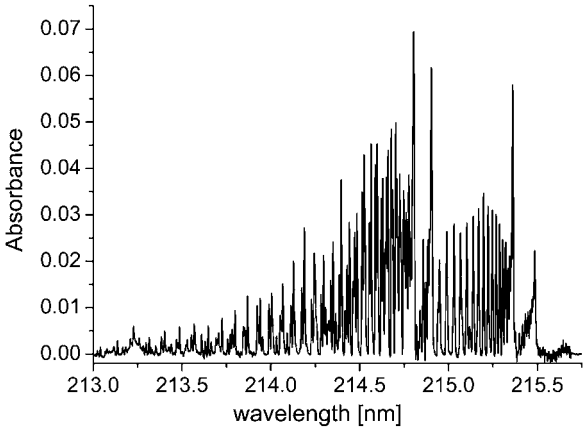

Fig. 2. High-resolution absorption spectrum of NO, gained by heating 5.6 µg nitrate (as nitric acid) and 68 µg lanthanum (as $LaCl_3$) in a graphite furnace.

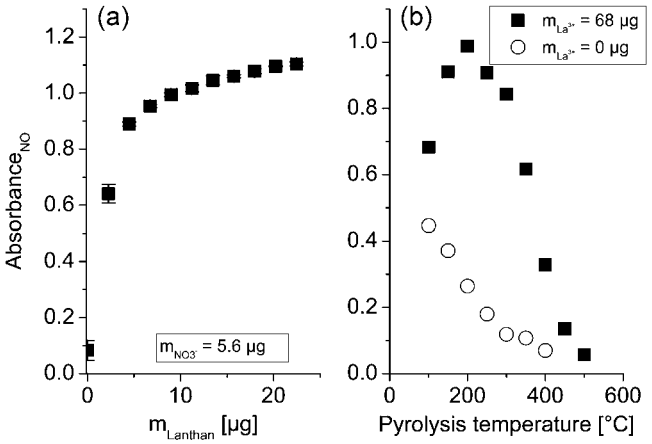

Fig. 3. Impact of (a) the lanthanum mass on the signal sensitivity of NO formed of HNO_3 at $m_{NO_3^-} = 5.6$ µg and (b) the pyrolysis temperature on the signal sensitivity of NO formed of HNO_3 at $m_{NO_3^-} = 5.6$ µg in the presence (filled markers) or absence (open markers) of 68 µg lanthanum (as $LaCl_3$).

[19]. The most sensitive peak at 214.803 nm was used as analyte signal. The underground correction was performed by means of static background correction with a reference measurement. Four wavelength ranges, 214.698–214.697 nm, 214.740–214.742 nm, 214.826–214.828 nm, and 214.922–214.927 nm, were chosen as markers for the polynomial baseline fitting after unwanted absorption structures were eliminated via the reference spectrum.

Huang et al. [19] reported a significant signal-depressing effect on the NO MAS caused by acids which have higher boiling temperatures than nitric acid. In the case of the real and synthetic etching solutions, it emerged that nitric acid is lost before the sample has dried properly. To overcome this problem, numerous modifiers were tested with regard to the NO absorption. Lanthanum was found to have the most prominent signal increasing effect, as shown in Fig. 3. An addition of 5 µg lanthanum (as $LaCl_3$) to the sample is sufficient to affect a rise of the sensitivity, followed by a less steep increase caused by the further addition of lanthanum. As shown in Fig. 3b, lanthanum immobilized the nitric acid, presumably through the formation of $La(NO_3)_3$, which decomposes at a temperature higher than the boiling point of nitric acid (126 °C vs. 83 °C). However, this effect seems to be only one reason for the efficiency of the lanthanum modifier, because sodium (one of the tested modifiers) was found to increase the signal less in spite of the much higher decomposition temperature of $NaNO_3$ (380 °C) compared to $La(NO_3)_3$ (126 °C). In the presence of the $LaCl_3$, the modifier sodium nitrate and nitric acid showed the same sensitivity for the NO MAS when the optimized furnace (Table 3) program was used. In conclusion, the described loss of HNO_3 during the drying of the sample [19] is avoided if the described approach is used.

Apart from other typical applications using lanthanum as modifier, significantly larger amounts are required for the present application. It emerged that, because of the precipitation of LaF_3 and $La_2(SiF_6)_3$, the presence of HF and H_2SiF_6 reduces the amount of free lanthanum ions necessary to retard the nitric acid. A mass of 68 µg lanthanum was found to be the optimum for the diluted samples used in the present work. Higher masses cause emissions of white smoke, leading to a diffuse light scattering and decreasing the light intensity.

The characteristic mass of 20 ng and a LOD of 96 ng nitrate can be reached with the presented method; the linear working range covers several orders of magnitudes up to 75 µg nitrate.

Neither spectral nor chemical interferences were found for aluminum, iron, calcium, magnesium, nickel, sodium, and copper, which represent the ions most likely present in an etching solution,

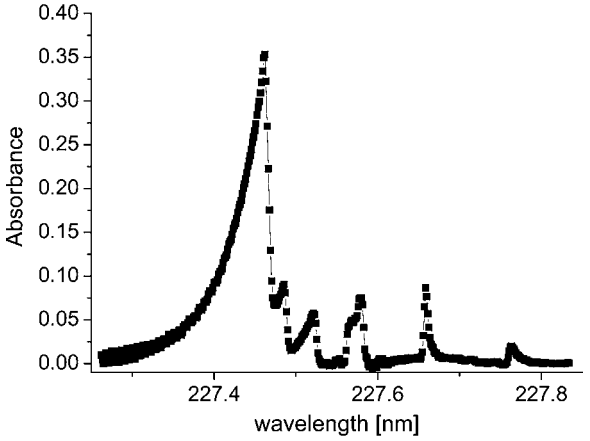

Fig. 4. High-resolution AlF molecular absorption spectrum in a graphite furnace at a pyrolysis temperature of 600 °C and a vaporization temperature of 2100 °C (assembled from three overlapping spectra; 7.5 ng fluoride, 8 μg aluminum, 8 μg barium).

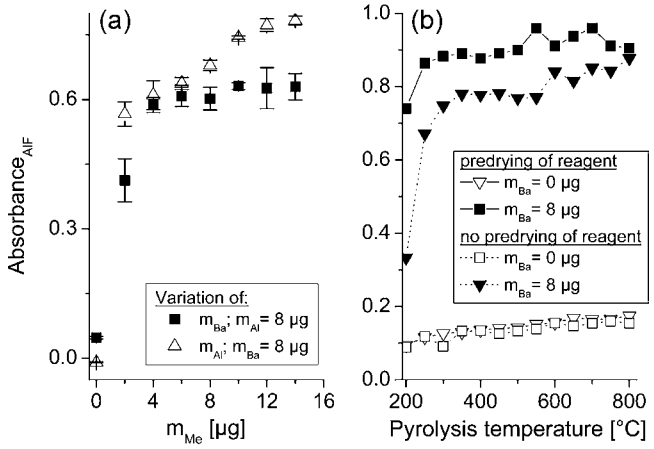

Fig. 5. Impact of (a) the reagent and modifier mass at a pyrolysis temperature of 600 °C and a vaporization temperature of 2100 °C and (b) of the pyrolysis temperature and injection regime (at m_{Al} = 8 μg and m_{Ba} = 8 μg or 0 μg) on the AlF molecular absorbance of 1.2 ng F (HF) at a vaporization temperature of 2100 °C.

if 100 ng of each metal (corresponding to 5 g L^{-1} in the undiluted sample) are added to the oven together with the sample.

3.1.3. Total fluoride determination

The diatomic molecule AlF shows pronounced structured absorption in the range of 227.40–227.80 nm, both in the flame [58] and in the graphite furnace (cf. Fig. 4). The most sensitive absorption band at the wavelength position of 227.46 nm ($X^1\Sigma^+ \rightarrow A^1\Pi$, ν = 1, 0, and $\Delta\nu$ = 0 [60]) was recorded as analyte signal. The background correction was performed by means of a reference spectrum to remove unwanted absorption structures; afterward, three pixel groups (227.367–227.323 nm, 227.531–227.535 nm, and 227.587–227.590 nm) served as markers for the polynomial baseline fitting.

The time-dependent signal of the AlF molecular absorption was found to depend on the composition of the etch solutions, i.e., it varied with different concentrations of HF and H_2SiF_6. In some cases, the time-dependent absorption signal was expanded so much that the signal integration took more than 15 s.

Barium (as $Ba(NO_3)_2$ solution) was found to be the best chemical modifier among the tested earth alkaline metals. The barium modifier generates a sharp absorption signal which lasts for no longer than 2 s, regardless of the composition of the analyte solution, which means that the integration time can be shortened to 5 s. A mass of 8 μg barium was chosen for the further application because of the almost constant signal found for this mass, as shown in Fig. 5a. Fig. 5a also displays the effect of the aluminum reagent mass at a constant mass of 8 μg barium. The AlF absorbance shows a steady increase in relation to the aluminum mass. However, the continuous background also increases. This indicates the formation of particles and causes a diffuse light scattering in the graphite tube. In consequence, this effect dramatically narrows the linear working range of the method. The best results for the AlF determination were found for 8 μg of aluminum reagent.

The barium modifier causes a significant change in the optimum pyrolysis temperature, as depicted in Fig. 5b. The sensitivity of the AlF molecular absorption in presence of the barium modifier increases strictly up to a pyrolysis temperature of 350 °C and remains almost constant up to a temperature of 550 °C (Fig. 5b). It is particularly favorable if the reagent is dried separately for 3 s at 110 °C before the sample and modifier are added to the furnace (Table 3). Then, a maximum in sensitivity is found at pyrolysis temperatures of between 300 °C and 500 °C (Fig. 5b). If the modifier is dried together with the reagent, the sensitivity does not reach such a high level. The optimized furnace program, summarized in Table 3, consists of the separate pre-drying of the reagent and the subsequent addition of both, sample and the modifier. With this strategy, a characteristic mass of 13 pg fluoride, a LOD of 145 pg fluoride, and a linear range of up to 5 ng fluoride is yielded.

Interference studies were performed with an unrealistically high amount of 100 ng of each metal. 100 ng correspond to the unrealistically high concentration of approximately 5 kg L^{-1} in the undiluted sample. Neither chemical nor spectral interferences were found for copper, sodium, iron, or magnesium. For 100 ng nickel, a weak absorption line (λ = 227.467 nm) at the right wing of the AlF absorption peak is observed. However, this is irrelevant for the fluoride determination because this line is located outside of the integration width of the AlF signal. The addition of 100 ng of calcium enhances the AlF absorbance by a factor of 1.1; however, this effect is lost at 3.3 ng.

3.2. Application of the method to synthetic and real sample solutions

3.2.1. Silicon determination through atomic absorption of silicon

The concentrations of silicon determined by means of HR-CS AAS of silicon are in good agreement with the values measured using ICP-OES (cf. Table 6). Although the uncertainty of the HR-CS AAS method is higher than that of the ICP-OES method, it is sufficient for industrial applications. With regard to the real sample, both methods result in almost identical values for the silicon concentration of 33.3 ± 0.5 g kg^{-1} measured with ICP-OES and 33.4 ± 1.6 g kg^{-1} measured with HR-CS AAS.

3.2.2. Nitrate determination by means of NO MAS

The results of the nitrate determination in the synthetic etching solutions by means of high-resolution continuum source molecular absorption spectrometry (HR-CS MAS) of NO are in good agreement with the data obtained using ion chromatography done by [7] (cf. Table 7). The HR-CS MAS yields to higher RSDs than IC, however, this span is acceptable for industrial applications. As before, both methods result in almost identical values of 238.3 ± 3.1 g kg^{-1} (IC) and 234.1 ± 4.5 g kg^{-1} (HR-CS MAS) for the concentration of nitric acid in the real sample.

3.2.3. Total fluoride determination by means of MAS of AlF

The total fluoride concentrations measured with AlF HR-CS MAS and ion chromatography [7] are consistent, as shown in Table 8. The

Table 6
Results of silicon and H_2SiF_6 determination through ICP-OES and HR-CS AAS; recovery rate is calculated by means of division of *w* (HR-CS AAS) by *w* (ICP-OES).

Sample	ICP-OES			HR-CS AAS			Recovery [%]
	w_{Si} [g kg^{-1}]	$w_{H_2SiF_6}$ [g kg^{-1}]	Recovery [%]	w_{Si} [g kg^{-1}]	$w_{H_2SiF_6}$ [g kg^{-1}]	RSD [%]	
1	39.4	202.2	0.8	39.2	200.9	1.8	99.3
2	25.2	129.0	0.8	25.9	132.7	2.1	102.8
3	20.9	107.4	0.3	20.6	105.7	3.0	98.4
4	24.2	124.3	1.4	24.4	125.3	2.1	100.8
5	39.6	203.3	0.4	38.5	197.7	2.6	97.2
Real sample	33.3	171.0	1.4	33.4	171.1	4.9	100.1

Table 7
Results of nitrate and nitric acid determination through IC and HR-CS MAS; recovery rate is calculated by means of division of *w* (HR-CS MAS) by *w* (IC).

Sample	IC			HR-CS MAS			Recovery [%]
	$w_{NO_3^-}$ [g kg^{-1}]	w_{HNO_3} [g kg^{-1}]	RSD [%]	$w_{NO_3^-}$ [g kg^{-1}]	w_{HNO_3} [g kg^{-1}]	RSD [%]	
1	306.9	311.8	0.5	299.5	304.3	3.0	97.6
2	202.6	205.8	1.9	212.5	215.9	4.2	104.9
3	253.3	257.3	0.4	257.5	261.6	4.6	101.7
4	256.4	260.5	0.3	252.1	256.2	3.3	98.3
5	308.4	313.3	0.1	294.5	299.2	0.8	95.5
Real sample	238.3	242.2	1.3	234.1	237.8	1.9	98.2

precision of the HR-CS MAS was in the typical range already found for silicon and nitrate, which is not as good as the IC method but still tolerable for an industrial application. The working range of the method, which spans from 435 pg (3 times LOD) to 5 ng fluoride, requires a rather high dilution of the sample. Nonetheless, the presented method allows the fast, sufficiently precise, and robust total fluoride determination in etching solutions.

3.3. The acid concentrations

The concentrations of H_2SiF_6 and HNO_3 are directly derived from the atomic absorption of silicon (Table 6) and from the NO molecular absorption (Table 7), respectively. The precision and recovery of the calculated acid concentrations are directly determined by the figure of merits of the absorption measurements. In the present study, is the concentrations are calculated from three individual sample dilutions, each of them measured three times.

The concentration of HF has to be calculated from the difference between the total fluoride concentration and the fluoride concentration bound to H_2SiF_6, i.e., from the silicon concentration of one given etch solution, using the following equation (M - molar mass):

$$w_{HF} = \frac{M_{HF}}{M_{F^-}} \left(w_{F^-} - 6 \cdot w_{Si} \cdot \frac{M_{F^-}}{M_{Si}} \right) \quad (2)$$

This calculation was performed using the silicon determination through ICP-OES and the total fluoride measurement through IC, as well as the HR-CS AAS measurements of the silicon atom and the AlF molecular absorption. The obtained HF concentrations for both routes are summarized in Table 9.

In general, the determination of the HF concentration via the HR-CS AAS route yields higher concentrations than the ICP-OES/IC route (with exception of sample 1). Although, the HR-CS AAS method is not as precise as the ICP-OES/IC route, it meets all the demands of a successful industrial application.

The focal point was on sample 1 and the real etching solution. Both samples, characterized by a low HF concentration in the presence of a high H_2SiF_6 concentration, demonstrate the limitations of both methods, particularly the route via atom and molecular absorption. This drawback is mainly caused by the uncertainty of the total fluoride determination using AlF MAS. Although the relative uncertainty of these measurements is moderate, the absolute errors ($\Delta c_{F^-} = 1.0$–6.4 g kg^{-1}) are relatively high compared to the smaller uncertainties of the silicon determination ($\Delta c_{Si} = 0.5$–1.6 g kg^{-1}). Error propagation finally leads to the finding of deviations and uncertainties of a few percent, as shown in Table 9. If the molar ratio of hydrofluoric acid and total fluoride is smaller than 0.3, the uncertainty increases to an extremely high level. The calculated concentration of HF via the IC and ICP-OES route suffers from the same effect. However, the lower uncertainties in the determination of silicon and fluoride result in lower uncertainties for the calculated HF concentration. Nevertheless, the presented method is a fast and robust method to quantify HF in etching solutions.

None of the developed methods suffer from serious chemical or spectral interferences. The observed chemical interferences on the AlF molecular absorption and on the silicon atomic absorption become irrelevant because of the high dilution of the samples required.

Another aspect regarding the analysis of such etch solutions should be mentioned. The presented method is based on the essential precondition that silicon is entirely bound in form of

Table 8
Results of total fluoride determination through IC and HR-CS MAS; recovery rate is calculated by means of division of *w* (HR-CS MAS) by *w* (IC).

Sample	IC		HR-CS MAS		Recovery [%]
	w_F [g kg^{-1}]	RSD [%]	w_F [g kg^{-1}]	RSD [%]	
1	181.7	0.5	177.3	3.5	97.6
2	183.6	1.8	187.9	2.1	102.4
3	150.8	0.6	151.6	2.1	100.6
4	155.0	0.2	159.0	0.6	102.5
5	221.2	0.1	220.8	2.1	99.8
Real sample	170.9	1.0	173.9	3.7	98.2

Table 9
Results of calculation of hydrofluoric acid concentration using the concentrations of silicon – and total fluoride. Comparison of applications via ICP-OES/IC and HR-CS MAS/HR-CS AAS; recovery rate is calculated by means of division of *w* (HR-CS AAS and MAS) by *w* (IC and ICP-OES).

Sample	IC and ICP-OES		HR-CS AAS and MAS		Recovery rate [%]
	w_{HF} [g kg^{-1}]	RSD [%]	w_{HF} [g kg^{-1}]	RSD [%]	
1	24.0	7.1	20.3	33.4	84.5
2	86.0	3.9	87.6	4.9	101.8
3	69.5	1.3	71.8	4.9	103.4
4	62.6	2.5	66.1	3.7	105.6
5	66.7	1.3	71.1	7.5	106.7
Real sample	37.8	6.9	40.8	19.4	108.0

H_2SiF_6. In fact, this has been proven by several studies. Neither the non-aqueous [5] nor the aqueous [6] acid–base titration methods showed any differences between synthetic etch solutions (manually prepared from HF, HNO_3, and H_2SiF_6) or etch solutions generated by the dissolution of silicon. An identical behavior has been verified by another independent method: The precipitation of H_2SiF_6 as K_2SiF_6 and the subsequent analysis of the mother solution by ion chromatography and ICP-OES, as described in detail in Ref. [7]. However, significant differences occur if the H_2SiF_6 used contains "extra" silicon in the form of dissolved SiO_2 as in the case of H_2SiF_6 from some commercial suppliers. Such H_2SiF_6 with "extra" Si must not be used for the development of analytical procedures or for calibration. Method [7] is well suited to quantify this extra amount. Finally, we have identified one case in which real etch solutions can contain more silicon than expected [61]. A recent study shows that Eq. (1) is only a simplified description of the etching process. It is possible to over-saturate etch solutions with silicon so that a molar silicon to fluorine ratio of 1:5 is obtained as quantitatively determined by method [7]. However, this is not relevant for any industrial etching process.

4. Conclusion

High-resolution continuum source absorption spectrometry allows the quantification of nitric acid, hexafluosilicic acid, and hydrofluoric acid using a single analytical instrument. The same instrumentation can be used to quantify traces of metal ions, which are known to accumulate in used etching solutions of the photovoltaic industry. Consequently, for the first time, the relevant constitution of an etching solution can be determined with a single analytical instrument. The presented method is characterized by minimal sample preparation (only dilution), a minimum effort of manpower, simple calibration with aqueous standards, and by its robustness against chemical and spectral interferences. The sample preparation only involves the preparation of three different dilutions of the concentrated acid mixture. The analytical results are in good agreement to other established methods based on IC and ICP-OES measurements. The method based on IC and ICP-OES requires the analysis of one sample by two different analytical instruments and is therefore more complex (different dilution, different standards etc.) and more time consuming. The developed analytical route yields to results of good precision and acceptable uncertainties for the three acids. In spite of the higher uncertainties compared to the IC/ICP-OES, the method of etch bath constituents analysis by means of atom and molecular absorption measurements fulfills all demands of an industrial application. The limit of the method was found for low HF concentrations in the presence of high concentrations of H_2SiF_6.

References

[1] H. Robbins, B. Schwartz, J. Electrochem. Soc. 106 (505) (1959) 508.
[2] M. Steinert, J. Acker, A. Henßge, K. Wetzig, J. Electrochem. Soc. 152 (2005) C843–C850.
[3] M. Steinert, J. Acker, M. Krause, S. Oswald, K. Wetzig, J. Phys. Chem. B 110 (2006) 11377–11382.
[4] W. Weinreich, J. Acker, I. Gräber, Semicond. Sci. Technol. 21 (2006) 1278–1286.
[5] A. Henßge, J. Acker, Talanta 73 (2007) 220–226.
[6] A. Henßge, J. Acker, C. Müller, Talanta 68 (2006) 581–585.
[7] J. Acker, A. Henßge, Talanta 72 (2007) 1540–1545.
[8] M. Zimmer, A. Oltersdorf, J. Rentsch, Talanta 80 (2009) 499–503.
[9] M. Zimmer, A. Oltersdorf, M. Meded, E. Kirchgässner, H. Furtwängler, S. Eigner, J. Rentsch, 22nd European Photovoltaic Solar Energy Conference and Exhibition, Milan, Italy, 07 September, 2007, 2007.
[10] M. Zimmer, K. Birmann, J. Hilgert, J. Rentsch, 24th European Solar Energy Conference and Exhibition, Hamburg, Germany, 25 September, 2009, 2009.
[11] M. Zimmer, A. Oltersdorf, E. Kirchgässner, J. Rentsch, 23rd European Photovoltaic Solar Energy Conference and Exhibition, Valencia, Spain, 05 September, 2008, 2008.
[12] U. Heitmann, H. Becker-Ross, S. Florek, M.D. Huang, M. Okruss, J. Anal. At. Spectrom. 21 (2006) 1314–1320.
[13] H. Gleisner, B. Welz, J.W. Einax, Spectrochim. Acta Part B 65 (2010) 864–869.
[14] H. Gleisner, J.W. Einax, S. Morés, B. Welz, E. Carasek, J. Pharm. Biomed. Anal. 54 (2011) 1040–1046.
[15] M.D. Huang, H. Becker-Ross, S. Florek, U. Heitmann, M. Okruss, Spectrochim. Acta Part B 63 (2008) 566–570.
[16] M.D. Huang, H. Becker-Ross, S. Florek, U. Heitmann, M. Okruss, B. Welz, Spectrochim. Acta Part B 64 (2009) 697–701.
[17] M. Resano, J. Briceño, M.A. Belarla, J. Anal. At. Spectrom. 24 (2009) 1343–1354.
[18] Z. Kowalewska, Spectrochim. Acta Part B 66 (2011) 546–556.
[19] M.-D. Huang, H. Becker-Ross, S. Florek, U. Heitmann, M. Okruss, B. Welz, H.S. Ferreira, J. Anal. At. Spectrom. 25 (2010) 163–168.
[20] K. Dittrich, Anal. Chim. Acta 111 (1979) 123–135.
[21] K. Dittrich, B. Vorberg, Chem. Anal. (Warsaw) 5 (1983) 539–555.
[22] K. Dittrich, B. Vorberg, J. Funk, V. Beyer, Spectrochim. Acta Part B 39 (1984) 349–363.
[23] K. Dittich, B. Hanisch, H.-J. Staerk, Fresenius Z. Anal. Chem. 324 (1986) 497–506.
[24] K.-I. Tsunoda, H. Haraguchi, K. Fuwa, in: H. Tsunoda, M.-H. Yu (Eds.) Studies in Environmental Science 27 (1986) 15–23 (Elsevier Science Publishers B.V., Amsterdam).
[25] K.-I. Tsunoda, H. Haraguchi, Keiichiro Fuwa, Spectrochim. Acta Part B 35 (1980) 715–729.
[26] K. Fuwa, H. Haraguchi, K.-I. Tsunoda, Proceedings on the 9th International Conference on Atomic Spectroscopy and 22nd Colloquium Spectroscopicim International, IUPAC Symposium Series, Tokyo, Japan 4–9 September, 1981, Pergamon Press, Oxford, 1982, pp. 119–129.
[27] K. Tsunoda, H. Haraguchi, K. Fuwa, Spectrochim. Acta Part B 40 (1985) 1651–1661.
[28] M.R. Shepard, B.T. Jones, D.J. Butcher, Appl. Spectrosc. 52 (1998) 430–437.
[29] K. Dittrich, V.M. Shkinev, B.V. Spivakov, Talanta 32 (1985) 1019–1022.
[30] K.-I. Tsunoda, K. Chiba, H. Haraguchi, C.L. Chakrabarti, K. Fuwa, Can. J. Spectrosc. 27 (1982) 94–99.
[31] D.A. Katskov, R.M. Mofolo, P. Tittarelli, Spectrochim. Acta Part B 55 (2000) 1577–1590.
[32] K. Dittrich, B. Vorberg, Anal. Chim. Acta 140 (1982) 237–248.
[33] G. Cobo, M. Gomez, C. Camara, M.A. Palacios, Mikrochim. Acta 110 (1993) 103–110.
[34] M. Gomez Gomez, M.A. Palacios Corvilio, C.C. Rica, Analyst 113 (1988) 1109–1112.
[35] M. Gomez, I. Rodriguez, C. Camara, M.A. Palacios, Analyst 115 (1990) 553–557.
[36] M. Gomez Gomez, A. Palacios Corvillo, C. Camara Rica, Analysis 19 (1991) 141–144.
[37] M.A. Palacios Corvillo, M. Gomez Gomez, C. Camara Rica, Talanta 37 (1990) 719–724.
[38] S. Fujimori, K. Itai, H. Tsunoda, Fluoride 17 (1984) 27–35.
[39] K. Itai, H. Tsunoda, M. Ikeda, Anal. Chim. Acta 171 (1985) 293–301.
[40] D.J. Butcher, Microchem. J. 48 (1993) 303–317.
[41] É.L. de Moraes Flores, J.S. Barin, É.M. de Moraes Flores, V.L. Dressler, Spectrochim. Acta Part B 62 (2007) 918–923.
[42] M.A. Fender, D.J. Butcher, Anal. Chim. Acta 315 (1995) 167–176.
[43] K. Tsunoda, K. Fujiwara, K. Fuwa, Anal. Chem. 49 (1977) 2035–2039.
[44] P. Venkateswarlu, Anal. Chim. Acta 262 (1992) 33–40.
[45] P. Venkateswarlu, L.D. Winter, R.A. Prokop, D.F. Hagen, Anal. Chem. 55 (1983) 2232–2236.
[46] P. Venkateswarlu, J.A. Balckwell, K. Jewell, G.W. Kirsch, J. AOAC Int. 75 (1992) 672–677.
[47] P. Venkateswarlu, M.A. Lacroix, G.W. Kirsch, Microchem. J. 48 (1993) 78–85.
[48] K. Chiba, K.-I. Tsunoda, H. Haraguchi, K. Fuwa, Anal. Chem. 52 (1980) 1582–1585.
[49] A. Takatsu, K. Chiba, M. Ozaki, K. Fuwa, H. Haraguchi, Spectrochim. Acta Part B 39 (1984) 365–370.
[50] K. Tsunoda, K. Chiba, H. Haraguchi, K. Fuwa, Anal. Chem. 51 (1979) 2059–2061.
[51] A. Nishida, M. Niwa, Shigaku 72 (1984) 871–881.
[52] T. Sugimura, M. Tomita, Y. Kaneko, J. Dent. Health 37 (1987) 508–509.
[53] H. Osada, Y. Iijima, T. Katayama, J. Dent. Health 39 (1989) 648–656.
[54] B. Yang, Y. Shi, Lihua Jianyan, Huaxue Fence 30 (1994) 74–77.
[55] B. Welz, F.G. Lepri, R.G.O. Araujo, S.L.C. Ferreira, M.-D. Huang, M. Okruss, H. Becker-Ross, Anal. Chim. Acta 647 (2009) 137–148.
[56] K. Dittrich, Prog. Anal. At. Spectrosc. 3 (1980) 209–275.
[57] K. Dittrich, CRC Crit. Rev. Anal. Chem. 16 (1986) 223–279.
[58] B. Welz, H. Becker-Ross, S. Florek, U. Heitmann, High-Resolution Continuum Source AAS, Wiley VCH, Weinheim, 2005.
[59] B. Welz, M. Sperling, Atomabsorptionsspektrometrie 4. Neubearbeitete Auflage, Wiley VCH, Weinheim, 1997.
[60] PLASUS SpecLine Datenbase, PLASUS Ingenieurbüro, Königsbrunn, Version 1.32.
[61] J. Acker, M. Steinert, V. Hoffmann, in preparation.